Available online at www.sciencedirect.com

ScienceDirect

Advances in Space Research xxx (2014) xxx–xxx

ADVANCES IN SPACE RESEARCH (a COSPAR publication)

www.elsevier.com/locate/asr

Improved ZEM/ZEV feedback guidance for Mars powered descent phase

Liuyu Zhou, Yuanqing Xia *

School of Automation, Beijing Institute of Technology, Beijing 100081, China

Received 19 December 2013; received in revised form 6 June 2014; accepted 13 August 2014

Abstract

An improved zero-effort-miss (ZEM) and zero-effort-velocity (ZEV) optimal feedback guidance algorithm is proposed in this paper for Mars powered descent phase, which has taken into account the no-subsurface constraints when designing the guidance law. Detailed descriptions have been given to this algorithm. The main advantage of this optimal guidance law is that it can successfully avoid collision to the Martian surface, at the same time preserving high landing precision and fuel optimality. For future Mars landing mission, the thrust-limited engine is most likely to be used. We propose a simulation method to study and determine the optimal final time which can minimize the fuel usage while ensuring precision landing and no-subsurface constraints. Monte Carlos are run to test the robustness and reliability of the improved and original guidance algorithms which show the superiority of the improved guidance law in preventing collision to the surface over the original one.

Keywords: ZEM/ZEV; Optimal guidance law; No-subsurface; Fuel-optimal; Precision landing

1. Introduction

Landing on Mars has been a hot research area in recent years. Many efforts have been made to it, such as the Viking, MPF, Spirit, Opportunity, Phoenix and MSL missions. The Mars entry, descent, landing (EDL) mission roughly includes four phases: the hypersonic entry phase, the subsonic parachute descent phase, the powered descent phase and the touchdown phase (Braun and Manning, 2007). The purpose of EDL mission is to deliver a vehicle to a desired place on Martian surface, which requires pinpoint landing. The Mars entry guidance is a tough problem due to the thinness and high-uncertainties of Martian atmosphere. The purpose of the entry guidance is to drive a vehicle to a desired parachute deployment site. The parachute is deployed and this parachute descent phase is totally uncontrolled. Then the parachute is discarded and the vehicle enters the powered decent phase, which will be discussed in this paper in detail. The landing guidance should be designed to satisfy the requirement of precision landing and fuel optimality. Many guidance laws and optimization methods have been proposed to address this problem. There are now many optimization softwares on the market, such as GPOPS, SNOPT, DIDO, TOMLAB and others. These softwares, which are based on various optimization methods, can automatically design an optimal trajectory which can satisfy the motion equations and various constraints at the same time.

Convex optimization method can also be used to design an optimal trajectory for Mars landing problem with many constraints (Acikmese and Ploen, 2007) and Blackmore et al. (2010) improved the convex optimization method to generate the minimum landing error trajectory when no feasible trajectory to the target exists. However, the

* Corresponding author. Tel.: +86 10 68914350; fax: +86 10 68914382.
E-mail addresses: liuyuzhou1@gmail.com (L. Zhou), xia_yuanqing@bit.edu.cn (Y. Xia).

http://dx.doi.org/10.1016/j.asr.2014.08.011
0273-1177/

powered decent guidance based on convex optimization is an open loop guidance which cannot be robust against disturbance, so an optimal feedback guidance law is needed for the landing mission which cannot only be fuel-optimal, but also achieve the precision landing requirement.

Ebrahimi et al. (2008) proposed a new optimal sliding mode guidance control law based on the zero-effort-miss (ZEM) and zero-effort-velocity (ZEV). The zero-effort-velocity(ZEV) error is a new concept proposed by Ebrahimi et al., which is analogous to the zero-effort-miss (ZEM) distance. ZEV is defined as the velocity error at the final time of the mission if no commanded acceleration is added to the vehicle since the current time. Ebrahimi et al. integrated this optimal guidance law with sliding-mode control for fixed-interval propulsive maneuvers with terminal velocity constraint (Ebrahimi et al., 2008). Furfaro et al. (2011) later modified this ZEM/ZEV optimal guidance law for a lunar precision landing mission which has shown robust performance against dispersions by simulation. But besides the precision landing and fuel-optimality requirement, the landing mission also requires no-subsurface flight. The ZEM/ZEV optimal guidance law does not account for this constraint, which may cause the vehicle to crash the ground following this guidance law. In order to rule out this possibility, Guo et al. (2013) proposed a waypoint-optimized zero-effort-miss/zero-effort-velocity feedback guidance for Mars landing, which can autonomously design an optimal waypoint using optimization approach during the powered descent phase if a subsurface flight is predicted. The designed waypoint is regarded as an intermediate target and the ZEM/ZEV algorithm is employed to reach it, and then reach the desired landing site.

The subsurface flight is most likely to happen if the landing site is behind the vehicle's initial position of powered descent phase which is a rare condition. By carefully designing the reference trajectory, this possibility can be reduced or even eliminated. So in most of the cases, the landing site is ahead of the vehicle's initial position. Besides, when the subsurface flight is predicted, whether the optimized waypoint can be found in a short period of time is also a crucial question.

So in this paper, we improve the zero-effort-miss (ZEM) and zero-effort-velocity (ZEV) optimal guidance law by taking the no-subsurface constraints into account when designing the guidance law. This is a trade-off between the precision landing, fuel optimality and no-subsurface requirements. We sacrifice a little landing precision to avoid the possibility of collision to the surface. According to the improved ZEM/ZEV optimal guidance law, the thrusting force can be automatically changed to prevent collision to the surface. Detailed descriptions have been given this algorithm. Besides, a new experimental study has been proposed to study the effect of different final time on the performance of the optimal feedback guidance regarding the fuel-optimal, pinpoint landing and no-subsurface requirement and the optimal final time is determined by trial. In simulation study, the target terminal altitude of the powered descent phase is set to 100 m, which is rational considering the altitude needed for the final touchdown phase. And the powered descent phase of the MSL mission also stops at 100 m to let the sky crane touchdown. Monte Carlos are run to test the robustness and reliability of the improved and original ZEM/ZEV guidance algorithms and to compare them in every aspect. Simulation results show that although the improved ZEM/ZEV guidance law has slightly less landing precision compared to the original one, it is definitely better in avoiding collision to the planet surface.

Sliding mode control (SMC) is a hot research topic in recent years. It can ensure stability, reliability and robustness in different control systems under actuator faults, external disturbances, model uncertainties and time-delay (Zhao et al., 2014; Wu et al., 2012; Liu et al., 2011; Lin et al., 2011; Wu et al., 2010; Zhang et al., 2010). So in Ebrahimi et al. (2008), Furfaro et al. (2011, 2013), the ZEM/ZEV optimal sliding-mode guidance law(OSG) which is a combination of the ZEM/ZEV optimal guidance law(OGL) and sliding-mode theory is discussed. However, from massive simulation, the OSG does not show any significant advantage in landing precision and fuel-optimality compared to OGL in this Mars power descent problem. Besides, the ZEM/ZEV optimal sliding-mode guidance law(OSG) is unpractical due to the chattering problem which is common in sliding-mode control. So we will not discuss OSG in this article.

This paper is organized as follows. The powered descent problem is formulated in Section 2. The improved optimal feedback guidance law with ZEM/ZEV is presented in Section 3. Section 4 gives simulation study and some discussions. Finally, some concluding remarks are given in Section 5.

2. Problem formulation

2.1. Equations of motion

During the powered descent phase, the vehicle's altitude is only within a few kilometers and its velocity is also very low. So the aerodynamic drag and lift forces can be neglected. The equations of motion during the powered descent phase for a Mars lander can be described by

$$\dot{\mathbf{r}} = \mathbf{v} \tag{1}$$

$$\dot{\mathbf{v}} = \mathbf{g} + \mathbf{a} \tag{2}$$

$$\mathbf{a} = \frac{\mathbf{T}}{m} \tag{3}$$

$$\dot{m} = -\frac{|\mathbf{T}|}{c} = -\frac{nkT_m \cos\theta}{I_{sp} g_e} \tag{4}$$

where $\mathbf{r}$ and $\mathbf{v}$ are the position and velocity vectors, $\mathbf{a}$ is the control acceleration provided by the thrusters, $\mathbf{T}$ is the thrusting force vector, m is the vehicle mass, and $\mathbf{g}$ is the gravitational acceleration vector acting on the vehicle. During the powered descent phase, $\mathbf{g}$ is considered to be

Please cite this article in press as: Zhou, L., Xia, Y. Improved ZEM/ZEV feedback guidance for Mars powered descent phase. J. Adv. Space Res. (2014), http://dx.doi.org/10.1016/j.asr.2014.08.011

constant due to the little variation of altitude. These vectors are all 3×1 column vectors expressed in a nonrotating inertial reference frame with its origin at the target landing site of Mars (Guo et al., 2013). The surface fixed reference frame is shown in Fig. 1. It is shown that the thrusting force vector $\mathbf{T}$ can be expressed as

$$\mathbf{T} = [T_x\ T_y\ T_z]^{\mathrm{T}} = \begin{bmatrix} |\mathbf{T}|\cos\alpha\sin\sigma \\ |\mathbf{T}|\cos\alpha\cos\sigma \\ |\mathbf{T}|\sin\alpha \end{bmatrix} = \begin{bmatrix} nkT_m\cos\theta\cos\alpha\sin\sigma \\ nkT_m\cos\theta\cos\alpha\cos\sigma \\ nkT_m\cos\theta\sin\alpha \end{bmatrix} \quad (5)$$

where $|\mathbf{T}| = nkT_m\cos\theta$ represents the two-norm of vector $\mathbf{T}$, which is the magnitude of the thrusting force. n is the number of identical thrusters. k is the throttle level of each thruster and T_m is the maximum available thrust magnitude. θ is the cant angle of the thrusters to net thrust direction (shown in Fig. 1). α is the thrust angle defined as the angle between the thrusting force $\mathbf{T}$ and the horizontal plane. And σ is the thrust roll angle which is the angle between the projection of $\mathbf{T}$ on the horizontal plane and the downrange direction. α and σ are also shown in Fig. 1. $\dot{m}$ is the negative mass flow rate and $c = I_{sp}g_e$ is the engine exhaust velocity with I_{sp} and g_e representing the impulse of the thrusters and earth gravitational acceleration respectively.

2.2. Constraints

During the powered descent phase, the lander has a path constraints with the boundary conditions as follows (Guo et al., 2013):

$$\mathbf{r}(t_0) = \mathbf{r}_0 = [x_0\ y_0\ z_0]^{\mathrm{T}}, \quad \mathbf{r}(t_f) = \mathbf{r}_f = [x_f\ y_f\ z_f]^{\mathrm{T}} \quad (6)$$

$$\mathbf{v}(t_0) = \mathbf{v}_0 = [\dot{x}_0\ \dot{y}_0\ \dot{z}_0]^{\mathrm{T}}, \quad \mathbf{v}(t_f) = \mathbf{v}_f = [\dot{x}_f\ \dot{y}_f\ \dot{z}_f]^{\mathrm{T}} \quad (7)$$

In addition, the landing guidance law should also ensure that the lander will stay above the Martian surface all the time during the powered descent phase in order to avoid collision with the surface of Mars, which is a precondition for a safe and successful landing. The altitude constraint can be expressed as

$$h = A\mathbf{r} \geqslant 0, \quad \text{for} \quad t_0 \leqslant t \leqslant t_f \quad (8)$$

where $A = [0\ 0\ 1]$.

There are two types of spacecraft engines – power-limited and thrust-limited engines. But for Mars landing mission, thrust-limited engine is most likely to be used. So only thrust-limited engine will be considered in this paper. And the engine exhaust velocity of the thrust-limited engine is fixed at a constant value. Theoretically, the throttle level of the thrust-limited engine is between 0 to 1, but in real practice, there is constraints on throttle level. In this paper, the constraint on throttle level is set between 0.3 to 0.8, which is the same as that in Acikmese and Ploen (2007). So the thrust magnitude is constrained as

$$0.3T_m \leqslant |\mathbf{T}| \leqslant 0.8T_m \quad (9)$$

where T_m is the maximum available thrust magnitude. So the thrust magnitude constraint will form a control saturation problem for $\mathbf{a}$.

2.3. Zero-effort errors

The zero-effort miss at time t, ZEM(t), is the distance (vector) that the vehicle will miss its target at the final time t_f with no acceleration command exerting on the vehicle after the current time t. Similarly, the zero-effort velocity error at time t, ZEV(t), is the error of velocity (vector) at the final time t_f if no acceleration command exerts on the vehicle after the current time t. Therefore,

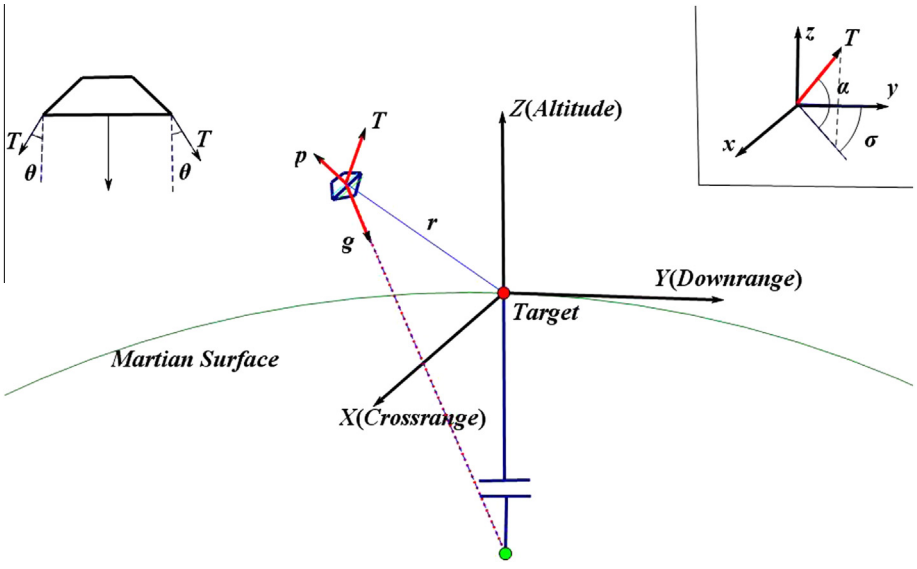

Fig. 1. Surface fixed reference frame.

Please cite this article in press as: Zhou, L., Xia, Y. Improved ZEM/ZEV feedback guidance for Mars powered descent phase. J. Adv. Space Res. (2014), http://dx.doi.org/10.1016/j.asr.2014.08.011

$$\mathbf{ZEM}(t) = \mathbf{r}_f - \mathbf{r}(t_f), \quad \mathbf{a}(\tau) = 0, \quad \text{for} \quad t \leqslant \tau \leqslant t_f \tag{10}$$

$$\mathbf{ZEV}(t) = \mathbf{v}_f - \mathbf{v}(t_f), \quad \mathbf{a}(\tau) = 0, \quad \text{for} \quad t \leqslant \tau \leqslant t_f \tag{11}$$

where $\mathbf{r}_f$ and $\mathbf{v}_f$ are the desired final position and velocity of the lander. Considering that the gravitational acceleration $\mathbf{g}$ is the only acceleration exerting on the vehicle which is also assumed to be a constant value, the ZEM(t) and ZEV(t) can be simplified as Guo et al. (2013)

$$\mathbf{ZEM}(t) = \mathbf{r}_f - \left(\mathbf{r} + t_{go}\mathbf{v} + \frac{1}{2}t_{go}^2\mathbf{g}\right) \tag{12}$$

$$\mathbf{ZEV}(t) = \mathbf{v}_f - \left(\mathbf{v} + t_{go}\mathbf{g}\right) \tag{13}$$

where $t_{go} = t_f - t$ is the time-to-go before reaching the terminal state.

3. Improved optimal feedback guidance with ZEM/ZEV

For optimization problem, the classical performance index employed in Ebrahimi et al. (2008), Furfaro et al. (2011, 2013), Guo et al. (2013, 2011), Hawkins et al. (2011, 2012), Guo et al. (2013) is as follow

$$J = \frac{1}{2}\int_{t_0}^{t_f} \mathbf{a}^{\mathrm{T}}\mathbf{a}\ \mathrm{d}t \tag{14}$$

The Hamiltonian function is defined as

$$H = \frac{1}{2}\mathbf{a}^{\mathrm{T}}\mathbf{a} + \mathbf{p}_r^{\mathrm{T}}\mathbf{v} + \mathbf{p}_v^{\mathrm{T}}(\mathbf{g} + \mathbf{a}) \tag{15}$$

where $\mathbf{p}_r$ and $\mathbf{p}_v$ are the costate vectors associated with the position and velocity vectors, respectively.

In Steinfeldt et al. (2010) and D'Souza and An (1997), an additional term corresponding to the final time t_f is added to the classical performance index (14). This represents a trade-off between the minimum time problem and the minimum control effort problem.

However, the classical performance index and Hamiltonian function above do not take into account the altitude constraints in (8) which may cause the vehicle to crash the ground. In order to rule out this possibility, we propose a novel performance index which add a term corresponding to the altitude constraints in (8) to the classical performance index. The novel performance index is as follow

$$J = \frac{1}{2}\int_{t_0}^{t_f} (\mathbf{a}^{\mathrm{T}}\mathbf{a} - \lambda A\mathbf{r})\ \mathrm{d}t \tag{16}$$

where λ is a parameter which we design as follow

$$\lambda = \begin{cases} 0 & z > z_f \\ c & z \leqslant z_f \end{cases} \tag{17}$$

where c is a positive constant. The Hamiltonian function is then defined as

$$H = \frac{1}{2}\mathbf{a}^{\mathrm{T}}\mathbf{a} - \frac{1}{2}\lambda A\mathbf{r} + \mathbf{p}_r^{\mathrm{T}}\mathbf{v} + \mathbf{p}_v^{\mathrm{T}}(\mathbf{g} + \mathbf{a}) \tag{18}$$

Remark 1. Note that for the optimization problem, we want to minimize the performance index, also called the cost function, (14). The algorithm we will use to minimize the performance index with the help of Hamiltonian function will be discussed next. So if we add a term $-\lambda A\mathbf{r}$ to the performance index, when the altitude $z = A\mathbf{r}$ is below z_f, the performance index will become smaller because of an extra negative term $-\lambda A\mathbf{r}$. Due to the purpose of the algorithm - minimize the performance index, there will be an extra thrusting force acting on the vehicle automatically, which will make it to fly upwards, to make the extra term $-\lambda A\mathbf{r}$ become smaller, until the altitude reaches z_f.

As the gravitational acceleration $\mathbf{g}$ is assumed to be the constant value in this problem, the optimal control equation and costate equations are as follows

$$\frac{\partial H}{\partial \mathbf{a}} = 0 \Rightarrow \mathbf{a} = -\mathbf{p}_v \tag{19}$$

$$\dot{\mathbf{p}}_r = -\frac{\partial H}{\partial \mathbf{r}} = \frac{1}{2}\lambda A^{\mathrm{T}} \tag{20}$$

$$\dot{\mathbf{p}}_v = -\frac{\partial H}{\partial \mathbf{v}} = -\mathbf{p}_r \tag{21}$$

The solutions of the optimal control equation and costate equations are

$$\mathbf{p}_r = \mathbf{p}_r(t_f) - \frac{1}{2}\lambda A^{\mathrm{T}} t_{go}. \tag{22}$$

$$\mathbf{p}_v = -\frac{1}{4}\lambda A^{\mathrm{T}} t_{go}^2 + t_{go}\mathbf{p}_r(t_f) + \mathbf{p}_v(t_f) \tag{23}$$

$$\mathbf{a} = -\mathbf{p}_v = \frac{1}{4}\lambda A^{\mathrm{T}} t_{go}^2 - t_{go}\mathbf{p}_r(t_f) - \mathbf{p}_v(t_f) \tag{24}$$

Integrating the acceleration $\mathbf{a}$, the velocity and position vectors can be obtained as

$$\mathbf{v} = -\frac{1}{12}\lambda A^{\mathrm{T}} t_{go}^3 + \frac{1}{2}t_{go}^2\mathbf{p}_r(t_f) + t_{go}\mathbf{p}_v(t_f) - t_{go}\mathbf{g} + \mathbf{v}_f \tag{25}$$

$$\mathbf{r} = \frac{1}{48}\lambda A^{\mathrm{T}} t_{go}^4 - \frac{1}{6}t_{go}^3\mathbf{p}_r(t_f) - \frac{1}{2}t_{go}^2\mathbf{p}_v(t_f) + \frac{1}{2}t_{go}^2\mathbf{g} - t_{go}\mathbf{v}_f + \mathbf{r}_f \tag{26}$$

Combining (25) and (26) leads to

$$\mathbf{p}_r(t_f) = \frac{6(\mathbf{v}_f + \mathbf{v})}{t_{go}^2} + \frac{12(\mathbf{r} - \mathbf{r}_f)}{t_{go}^3} + \frac{1}{4}\lambda A^{\mathrm{T}} t_{go} \tag{27}$$

$$\mathbf{p}_v(t_f) = -\frac{2(2\mathbf{v}_f + \mathbf{v})}{t_{go}} - \frac{6(\mathbf{r} - \mathbf{r}_f)}{t_{go}^2} + \mathbf{g} - \frac{1}{24}\lambda A^{\mathrm{T}} t_{go}^2 \tag{28}$$

So the improved optimal guidance law can be obtained as

$$\mathbf{a} = \frac{6[\mathbf{r}_f - (\mathbf{r} + t_{go}\mathbf{v})]}{t_{go}^2} - \frac{2(\mathbf{v}_f - \mathbf{v})}{t_{go}} - \mathbf{g} + \frac{1}{24}\lambda A^{\mathrm{T}} t_{go}^2 \tag{29}$$

For a soft landing problem with $\mathbf{v}_f = 0$, the improved OGL has the following form

Please cite this article in press as: Zhou, L., Xia, Y. Improved ZEM/ZEV feedback guidance for Mars powered descent phase. J. Adv. Space Res. (2014), http://dx.doi.org/10.1016/j.asr.2014.08.011

Table 1
Initial perturbations.

Initial perturbations	Mean value	Standard dev.
Crossrange	0 m	50 m
Downrange	−2000 m	150 m
Altitude	1500 m	100 m
Velocity x	0 m/s	10 m/s
Velocity y	100 m/s	10 m/s
Velocity z	−75 m/s	5 m/s
Mass	1905 kg	30 kg

$$\mathbf{a} = \frac{6(\mathbf{r}_f - \mathbf{r})}{t_{go}^2} - \frac{4\mathbf{v}}{t_{go}} - \mathbf{g} + \frac{1}{24}\lambda A^{\mathrm{T}} t_{go}^2 \tag{30}$$

Substituting (12) and (13) into the above equation, we get the improved optimal feedback guidance law with ZEM/ZEV

$$\mathbf{a} = \frac{6}{t_{go}^2}\mathbf{ZEM} - \frac{2}{t_{go}}\mathbf{ZEV} + \frac{1}{24}\lambda A^{\mathrm{T}} t_{go}^2 \tag{31}$$

Remark 2. We can see from (29)–(31) that this improved optimal guidance law adds an extra term $\frac{1}{24}\lambda A^{\mathrm{T}} t_{go}^2$ to the original optimal guidance law (OGL). This is consistent with our design purpose of performance index (16), because when the altitude $z \leqslant z_f$, the term $\frac{1}{24}\lambda A^{\mathrm{T}} t_{go}^2$ becomes nonzero and is acted as an extra thrusting force on vehicle which helps it to fly upwards, avoiding collision to the planet surface.

4. Simulation results

4.1. Parameter design

In this paper, the parameters of the vehicle for simulation are mainly from Acikmese and Ploen (2007), which are as follows

$$\begin{aligned} &m_0 = 1905\ \text{kg}, \quad \mathbf{g} = [0\ 0\ -3.7114]^{\mathrm{T}}\ \text{m/s}^2 \\ &n = 6, \quad \theta = 27\ \text{deg} \\ &I_{sp} = 225\ \text{s}, \quad g_e = 9.807, \quad T_m = 3100\ \text{N} \end{aligned} \tag{32}$$

The initial position and velocity of the lander are given as follows (Acikmese and Ploen, 2007)

$$\mathbf{r}(t_0) = \mathbf{r}_0 = [0\ -2000\ 1500]^{\mathrm{T}}\ \text{m} \tag{33}$$

$$\mathbf{v}(t_0) = \mathbf{v}_0 = [0\ 100\ -75]^{\mathrm{T}}\ \text{m/s} \tag{34}$$

In this paper, the target terminal position and velocity are set as

$$\mathbf{r}(t_f) = \mathbf{r}_f = [0\ 0\ 100]^{\mathrm{T}}\ \text{m} \tag{35}$$

$$\mathbf{v}(t_f) = \mathbf{v}_f = [0\ 0\ 0]^{\mathrm{T}}\ \text{m/s} \tag{36}$$

The target terminal altitude is set to 100 m for the final touchdown phase to execute. If the target terminal position is set to the surface of Mars, the air flow of the engines will blow the dust up which may have a negative impact on the vehicle. The navigation system on the lander may be seriously damaged if the dust is blew up and covers the cameras. So in order to avoid this adverse situation, the powered descent phase should terminate at an altitude above the Martian surface. The Mars Science Laboratory (MSL) mission has designed a sky crane landing for the final touchdown phase, which has proven to be a good solution to this problem.

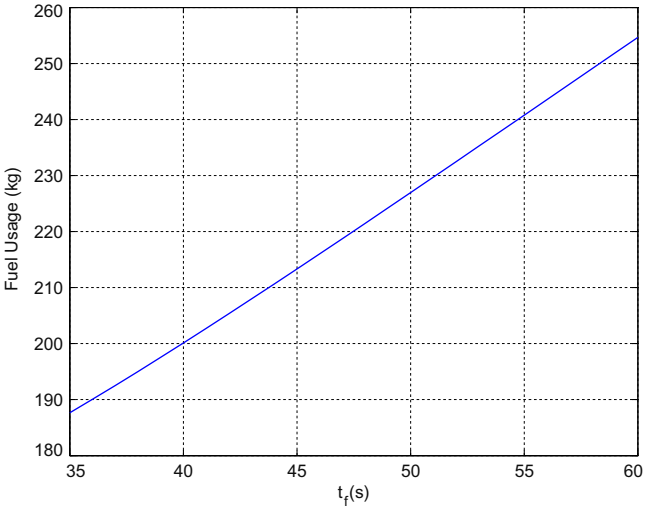

Fig. 2. Fuel usage for various t_f.

The initial perturbations are shown in Table 1 for Monte Carlo simulations.

4.2. Determination of optimal time-to-go

From (31), it is shown that the time-to-go $t_{go} = t_f - t$ has an important effect on the performance of the optimal feedback guidance laws (original and improved OGL). Unless the total time-to-go of the powered descent phase

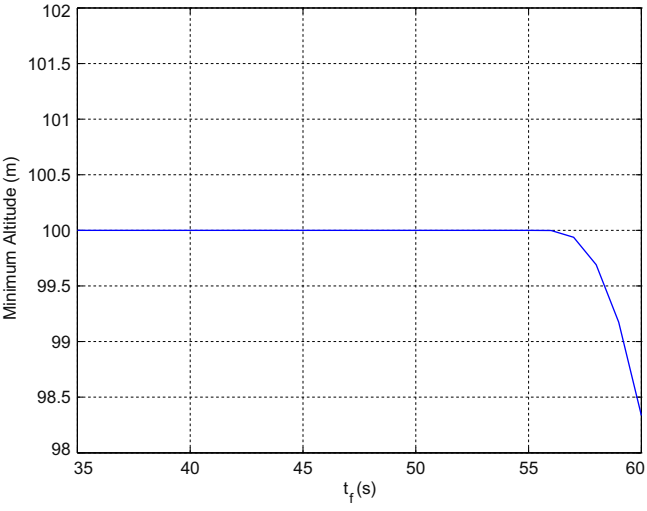

Fig. 3. Minimum altitude for various t_f.

Please cite this article in press as: Zhou, L., Xia, Y. Improved ZEM/ZEV feedback guidance for Mars powered descent phase. J. Adv. Space Res. (2014), http://dx.doi.org/10.1016/j.asr.2014.08.011

Table 2
Landing precision for various t_f.

Mean value vs t_f	30 s	35 s	40 s	45 s
Crossrange	0.1292 m	−0.0247 m	-1.0710×10^{-4} m	4.1191×10^{-6} m
Downrange	58.9524 m	1.7807 m	0.0149 m	1.1241×10^{-4} m
Altitude	23.3845 m	97.5814 m	99.9726 m	99.9997 m
Velocity x	0.0311 m/s	−0.0105 m/s	-6.3293×10^{-4} m	3.2170×10^{-4} m/s
Velocity y	13.9600 m/s	1.0585 m/s	0.0346 m/s	−0.0074 m/s
Velocity z	−16.5214 m/s	−1.4892 m/s	−0.0728 m/s	−0.0042 m/s
Mass	1742.4 kg	1718.7 kg	1703.9 kg	1690.8 kg

Table 3
Landing statistics with OGL.

Landing statistics	Mean value	Standard dev.
Crossrange	5.9124×10^{-6} m	8.0346×10^{-5} m
Downrange	1.3202×10^{-4} m	1.4106×10^{-4} m
Altitude	99.9998 m	3.9655×10^{-4} m
Velocity x	5.8410×10^{-4} m/s	0.0049m/s
Velocity y	−0.0071 m/s	0.0148 m/s
Velocity z	−0.0014 m/s	0.0330 m/s
Mass	1693.1 kg	28.4988 kg

Table 4
Landing statistics with improved OGL.

Landing statistics	Mean value	Standard dev.
Crossrange	1.7195×10^{-5} m	2.3863×10^{-4} m
Downrange	$1.0136 \times 10^{-}4$ m	5.3703×10^{-4} m
Altitude	99.9995 m	0.0027 m
Velocity x	4.2053×10^{-4} m/s	0.0057 m/s
Velocity y	−0.0070 m/s	0.0120 m/s
Velocity z	−0.0041 m/s	0.0618 m/s
Mass	1691.3 kg	27.0150 kg

is constrained, the time-to-go t_{go} in every guidance cycle can be determined to achieve the optimal performance in fuel consumption and precision landing. But this is not easy considering the large amount of time which will be spent on finding the optimal time-to-go. Guo et al. (2011) proposed a numerical method to calculate the optimal time-to-go for the power-limited engine. But for a thrust-limited engine, minimizing J (see (14)) does not mean minimizing the fuel usage, so the result obtained by the numerical method mentioned above is not the optimal time-to-go for the thrust-limited engine. As a result, the optimal ZEM/ZEV guidance laws discussed in this paper are not fuel-optimal in nature, but the fuel usage can be regarded as the performance measure of interest (Guo et al., 2011). In this section, the impact of time-to-go on the performance of the optimal guidance laws will be discussed and the optimal time-to-go of the Mars powered descent phase will be determined by trial. Note that in the following we will use the simulation results of the original OGL to study and determine the optimal time-to-go.

In order to find the optimal time-to-go which can minimize the fuel usage, the fuel usage for various t_f is shown in Fig. 2 below. From Fig. 2, it is shown that the fuel usage is

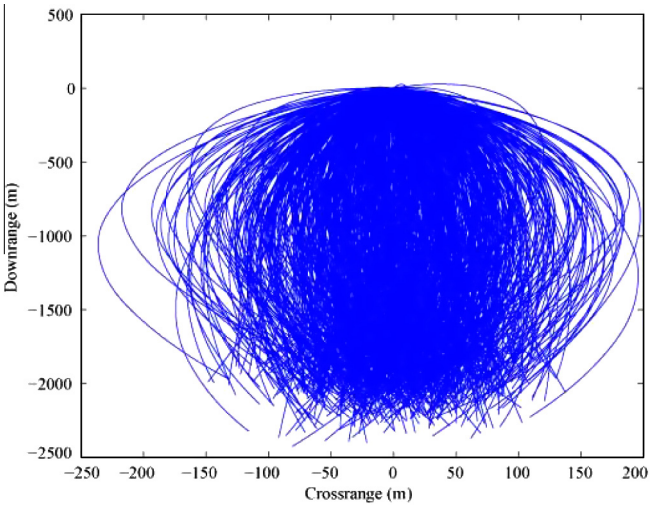

Fig. 4. Trajectories of OGL.

positive proportional to t_f. So the less time-to-go is, the less fuel will be consumed. But the optimal time-to-go cannot be too small considering the constraints on control forces. Besides, the no-subsurface constraint will also be used to find the optimal time-to-go. The minimum altitude in every trajectory for various t_f is shown in Fig. 3. From Fig. 3, we can see that when the final time t_f is greater than 57 s, the minimum altitude will be below 100 m, which is undesir-

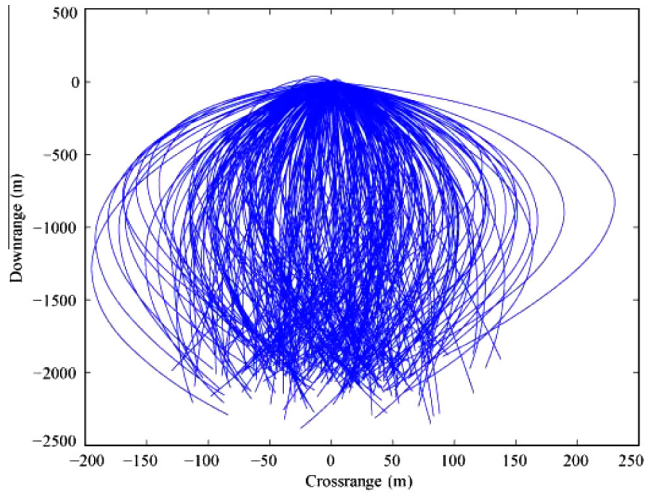

Fig. 5. Trajectories of improved OGL.

Please cite this article in press as: Zhou, L., Xia, Y. Improved ZEM/ZEV feedback guidance for Mars powered descent phase. J. Adv. Space Res. (2014), http://dx.doi.org/10.1016/j.asr.2014.08.011

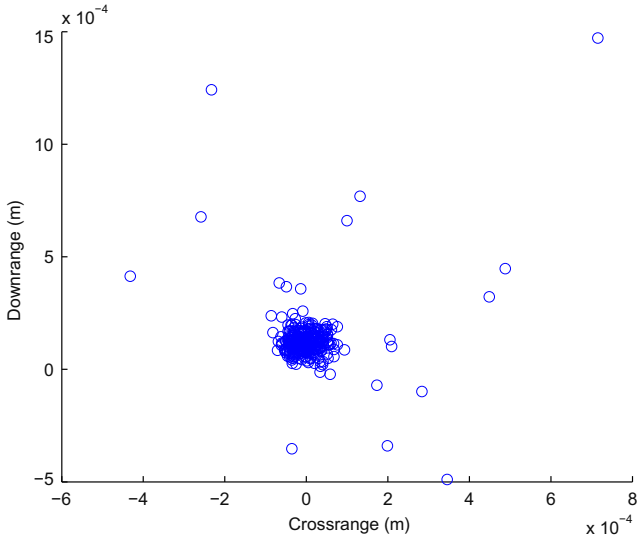

Fig. 6. Landing dispersion of OGL.

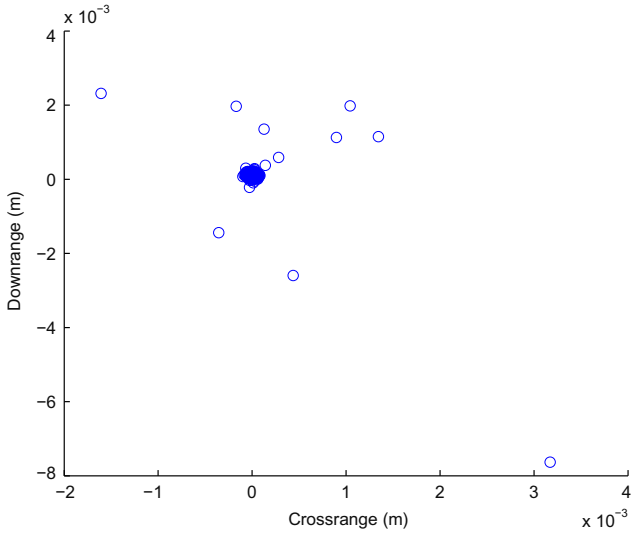

Fig. 7. Landing dispersion of improved OGL.

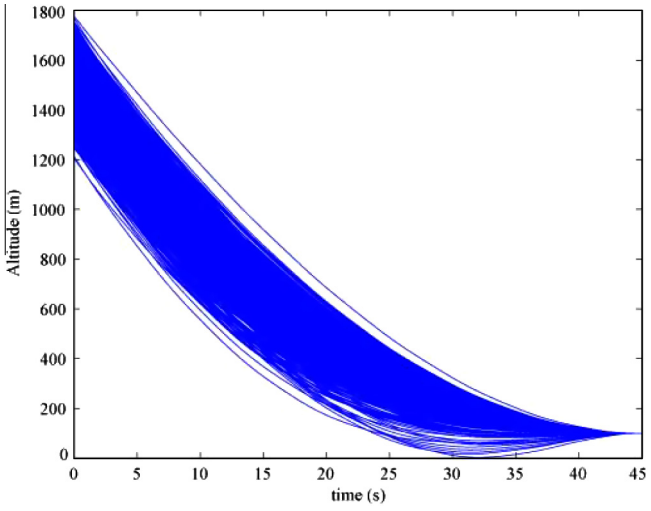

Fig. 8. Altitude vs time of OGL.

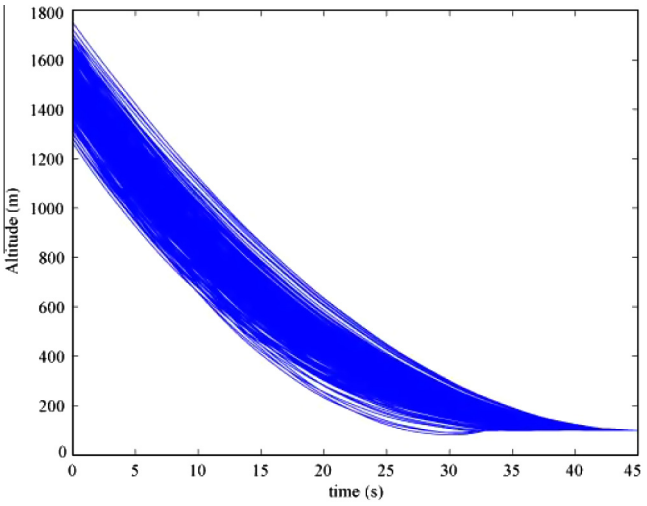

Fig. 9. Altitude vs time of improved OGL.

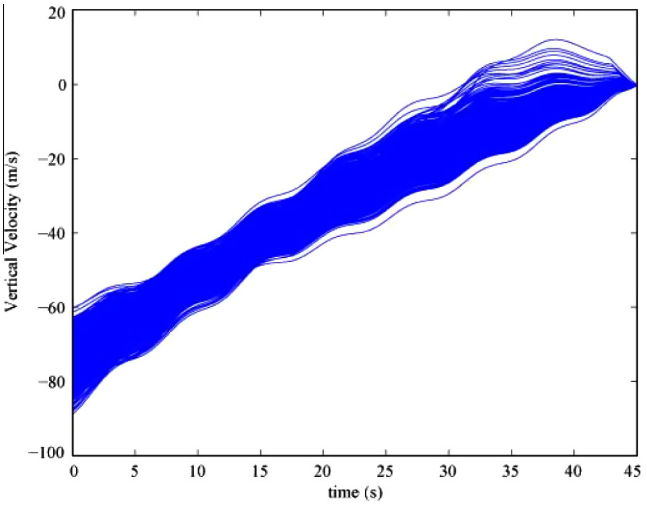

Fig. 10. Vertical velocity vs time of OGL.

able considering the greater chance of collision if the target site is at the Martian surface. So the final time t_f is better to set below 57 s.

Another problem that needs to be concerned is the precision landing requirement. If the time-to-go is set too low, the thrusting force will saturate, which may not satisfy the precision landing requirement. The landing precision for various t_f with initial perturbations(see Table 1) will be shown in Table 2 below.

The data above shows that when the final time t_f is below 40 s, the final velocity is greater than 1 m/s, which cannot satisfy the soft landing requirement. When the final time t_f is greater than 40 s, the landing precision is good enough to satisfy the requirement. The position and velocity errors have a magnitude at least of 10^{-3}. Besides, the final mass for various t_f agrees with the tendency shown in Fig. 2 that the fuel usage is direct proportional to the final time t_f. So in order to be fuel-optimal, the final time should be set between 40 s to 45 s.

Please cite this article in press as: Zhou, L., Xia, Y. Improved ZEM/ZEV feedback guidance for Mars powered descent phase. J. Adv. Space Res. (2014), http://dx.doi.org/10.1016/j.asr.2014.08.011

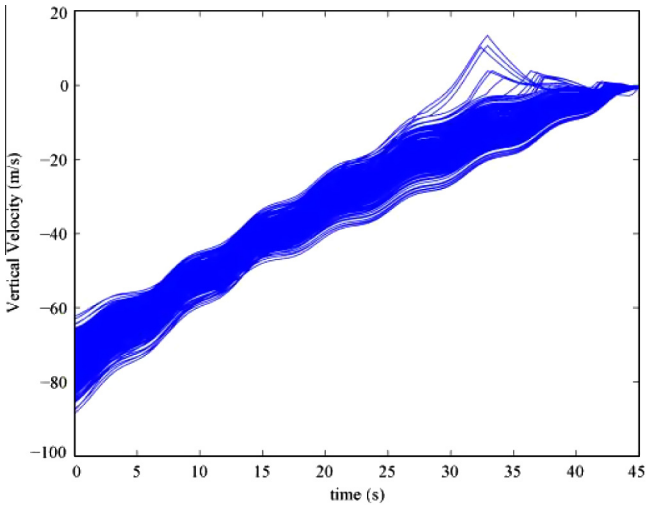

Fig. 11. Vertical velocity vs time of improved OGL.

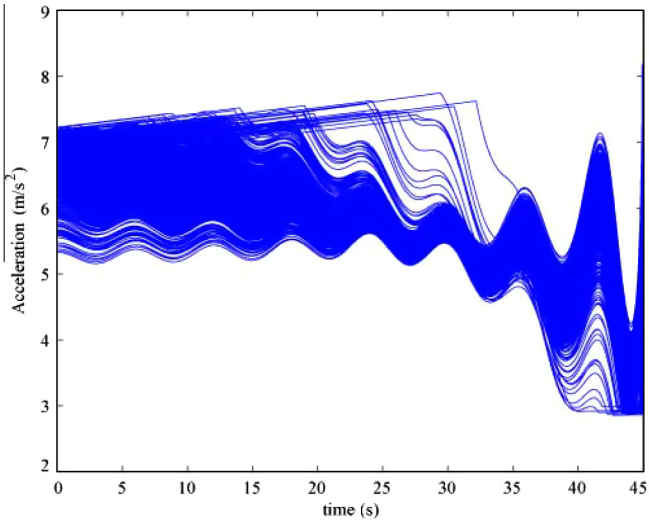

Fig. 12. Commanded acceleration vs time of OGL.

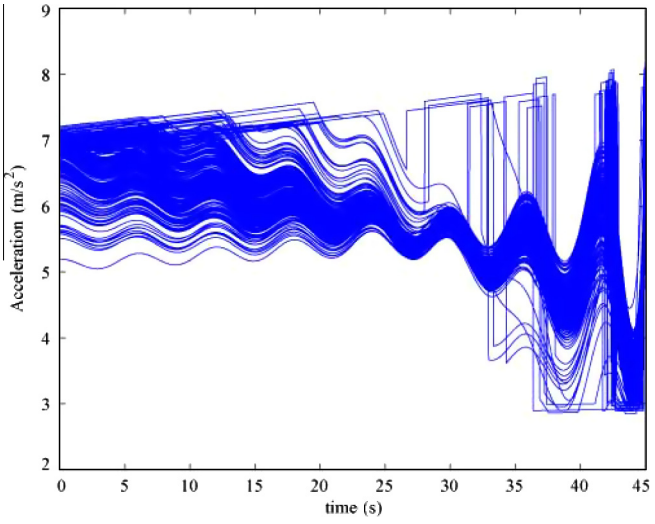

Fig. 13. Commanded acceleration vs time of improved OGL.

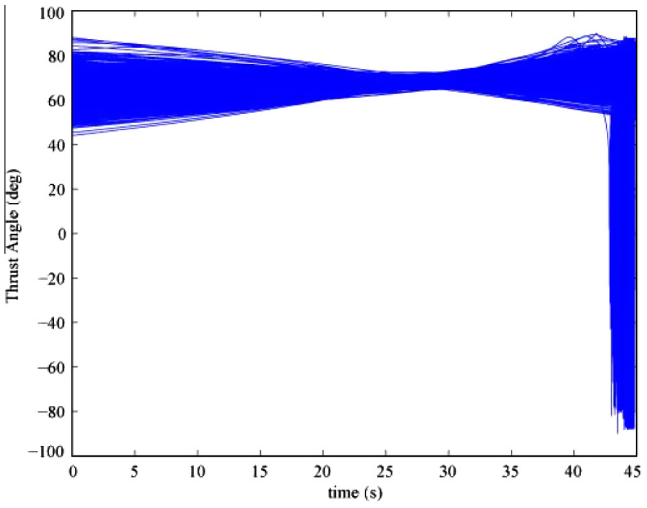

Fig. 14. Thrust angle vs time of OGL.

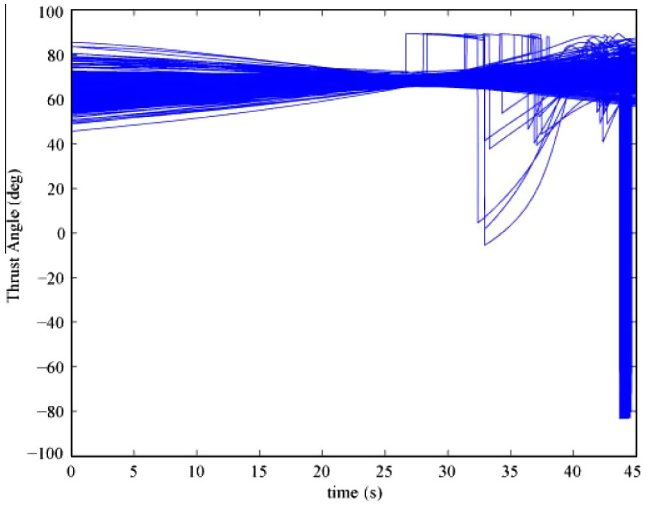

Fig. 15. Thrust angle vs time of improved OGL.

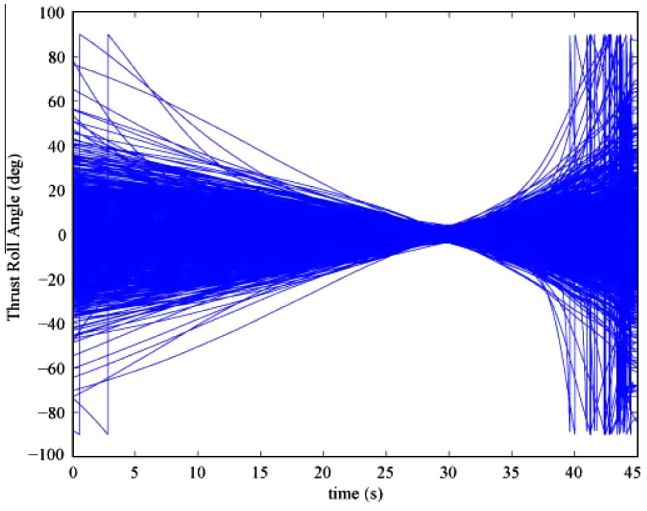

Fig. 16. Thrust roll angle vs time of OGL.

Please cite this article in press as: Zhou, L., Xia, Y. Improved ZEM/ZEV feedback guidance for Mars powered descent phase. J. Adv. Space Res. (2014), http://dx.doi.org/10.1016/j.asr.2014.08.011

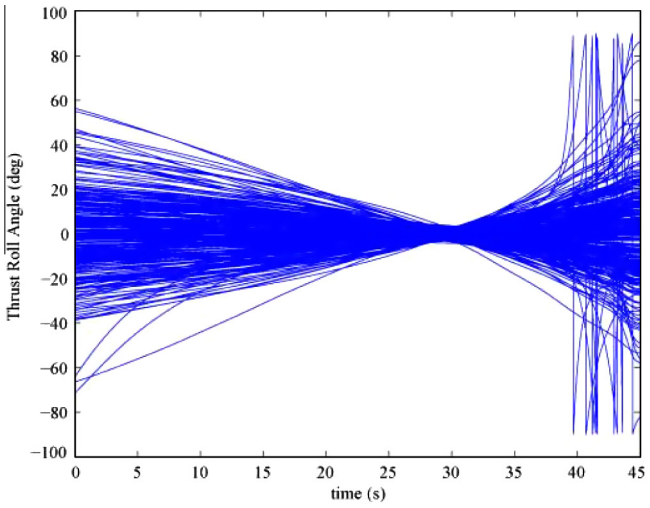

Fig. 17. Thrust roll angle vs time of improved OGL.

The final time t_f will be set to 45 s for the Monte Carlo simulation in the next subsection to leave some control margin for the assumed initial perturbations.

4.3. Monte Carlo simulations

In order to assess the robustness and reliability of the original and improved OGL and to compare them in every aspect, Monte Carlos with 300-dispersed cases, varying initial states and model errors, were run using Matlab simulation for the two guidance algorithms. The guidance cycle is set to 10 ms. The initial dispersions are listed in Table 1 for both two algorithms.

In addition, errors in mass, thrust, gravitational acceleration and wind influence will also be added in simulation as a perturbation $\mathbf{p}$ on the acceleration. $\mathbf{p}$ is assumed to be $\mathbf{p}(t) = \mathbf{P}\sin(\frac{\pi}{3}t)$, where $\mathbf{P} = 0.2\mathbf{a}$.

The landing statistics of the original OGL and improved OGL are shown in Tables 3 and 4. And the comparison of the original and improved OGL on trajectories, landing dispersions, altitude, vertical velocity, commanded acceleration, thrust angle and thrust roll angle are shown in Figs. 4–17.

As is shown in Tables 3 and 4, although the landing precision of the original OGL is slightly better than that of the improved one, it is neglectable considering the large size of the lander. So we can say that the original and improved OGL have almost identical performance in precision landing and fuel consumption. And the profiles of altitude, vertical velocity, commanded acceleration, thrust angle and thrust roll angle are nearly the same. This is reasonable considering the nature of the improved OGL proposed in this paper. Only when the altitude is below the desired final altitude, an additional term is added to the original optimal guidance law to let it fly upwards, avoiding collision to the ground. When the altitude is above the desired final altitude, the improved OGL is identical to the original one.

The main difference of the original and improved OGL lies in the altitude profiles. Fig. 8 shows that about one fifth of the cases have a minimum altitude below 100 m during the power descent phase. In some cases, the minimum altitude reaches 0 m, or even below 0 m. If we set the final altitude below 100 m, let's say 0 m – planet surface, in many cases the vehicle will crash the ground before reaching the target landing place. However, we can see from Fig. 9 that only several cases have a minimum altitude below 100 m during power descent and they are just slightly below 100 m. In most of the cases, the minimum altitude is just 100 m, which forms a horizontal straight line on 100 m as shown in Fig. 9. So this demonstrates that the improved optimal guidance law is effective in preventing subsurface flight, in other words, collision to the surface.

5. Conclusions

For Mars power descent problem, an improved optimal guidance law with ZEM/ZEV is proposed in this paper to address the altitude constraints. This method can be fuel-optimal, at the same time satisfying the precision landing and no-subsurface flight requirement. Besides, the optimal time-to-go has been studied and determined by simulation method. Simulation results show that both the original and improved optimal guidance law have robust and reliable performances under perturbations. And simulation also demonstrates the effectiveness of the improved OGL in avoiding collision to the planet surface.

Acknowledgement

The authors would like to thank the referees for their valuable and helpful comments which have improved the presentation. The work was supported by the National Basic Research Program of China (973 Program) (2012CB720000), the National Natural Science Foundation of China (61225015), Foundation for Innovative Research Groups of the National Natural Science Foundation of China (Grant No. 61321002), the Ph.D.Programs Foundation of Ministry of Education of China (20111101110012), and CAST Foundation (CAST201210).

References

Acikmese, B., Ploen, S.R., 2007. Convex programming approach to powered descent guidance for mars landing. J. Guidance Control Dyn. 30 (5), 1353–1366.

Blackmore, L., Acikmese, B., Scharf, D.P., 2010. Minimum-landing-error powered-descent guidance for Mars landing using convex optimization. J. Guidance Control Dyn. 33 (4), 1161–1171.

Braun, R.D., Manning, R.M., 2007. Mars exploration entry, descent, and landing challenges. J. Spacecraft Rockets 44 (2), 310–323.

D'Souza, C., 1997. An optimal guidance law for planetary landing. AIAA, 1997–3709.

Ebrahimi, B., Bahrami, M., Roshanian, J., 2008. Optimal sliding-mode guidance with terminal velocity constraint for fixed-interval propulsive maneuvers. Acta Astron. 62 (10–11), 556–562.

Furfaro, R., Selnick, S., Cupples, M.L., Cribb, M.W., 2011. Non-linear sliding guidance algorithms for precision lunar landing. In: 21st AAS/AIAA Space Flight Mechanics Meeting. AAS, pp. 11–167.

Furfaro, R., Gaudet, B., Wibben, D.R., Simo, J., 2013. Development of non-linear guidance algorithms for asteroids close-proximity operations, In: AIAA Guidance, Navigation, and Control (GNC) Conference, August 19–22, Boston, MA.

Guo, Y., Hawkins, M., Wie, B., 2011. Optimal feedback guidance algorithms for planetary landing and asteroid intercept. In: AAS/AIAA Astrodynamics Specialist Conference. AAS, pp. 11–588.

Guo, Y., Hawkins, M., Wie, B., 2013. Applications of generalized zero-effort-miss/zero-effort-velocity feedback guidance algorithm. J. Guidance Control Dyn.

Guo, Y., Hawkins, M., Wie, B., 2013. Waypoint-optimized zero-effort-miss/zero-effort-velocity feedback guidance for mars landing. J. Guidance Control Dyn. 36 (3).

Hawkins, M., Guo, Y., Wie, B., 2011. Guidance algorithms for asteroid intercept missions with precision targeting requirements, In: AAS/AIAA Astrodynamics Specialist Conference, 2011-531.

Hawkins, M., Guo, Y., Wie, B., 2012. ZEM/ZEV feedback guidance application to fuel-efficient orbital maneuvers around an irregular-shaped asteroid, In: AIAA Guidance, Control, and Navigation Conference, Minneapolis, Minnesota.

Lin, Z., Xia, Y., Shi, P., Wu, H., 2011. Robust sliding mode control for uncertain linear discrete systems independent of time-delay. Int. J. Innovative Comput. Inf. Control 7 (2), 869–881.

Liu, M., Shi, P., Zhang, L., Zhao, X., 2011. Fault tolerant control for nonlinear Markovian jump systems via proportional and derivative sliding mode observer. IEEE Trans. Circuits Syst. I: Regul. Pap. 58 (11), 2755–2764.

Steinfeldt, B.A., Grant, M.J., Matz, D.A., Braun, R.D., Barton, G.H., 2010. Guidance, navigation, and control system performance trades for mars pinpoint landing. J. Spacecraft Rockets 47 (1).

Wu, L., Shi, P., Gao, H., 2010. State estimation and sliding mode control of Markovian jump singular systems. IEEE Trans. Autom. Control 55 (5), 1213–1219.

Wu, L., Su, X., Shi, P., 2012. Sliding mode control with bounded L_2 gain performance of Markovian jump singular time-delay systems. Automatica 48 (8), 1929–1933.

Zhang, J., Shi, P., Xia, Y., 2010. Robust adaptive sliding mode control for fuzzy systems with mismatched uncertainties. IEEE Trans. Fuzzy Syst. 18 (4), 700–711.

Zhao, J., Jiang, B., Shi, P., He, Z., 2014. Fault tolerant control for damaged aircraft based on sliding mode scheme. Int. J. Innovative Comput. Inf. Control 10 (1), 293–302.

Please cite this article in press as: Zhou, L., Xia, Y. Improved ZEM/ZEV feedback guidance for Mars powered descent phase. J. Adv. Space Res. (2014), http://dx.doi.org/10.1016/j.asr.2014.08.011